E. Information Content of a Single Pass of Doppler Data from a Distant Spacecraft

T. W. Hamilton and W. G. Melbourne

1. Introduction

On a typical pass of two-way tracking of a distant spacecraft, the doppler frequency is continuously counted from the time of initial "lock" until the end of the pass. The cumulative count is read out at regular intervals, typically 1 min. The data are sometimes "compressed" by forming first differences from every Kth sample and dividing by KT_s, where T_s is the original readout or sampling interval. Such "doppler frequencies" are interpreted as the space probe radial velocity with respect to the tracking station.

On a planetary mission such as *Mariner IV*, over 200 passes containing more than 500 samples in each pass can easily be accumulated. It is desirable that each pass be "compressed" into a smaller set of numbers characterizing the *trajectory-determining* information—here we will not be concerned with the higher-frequency information content relating to system noise, spacecraft oscillations, and atmospheric effects. Besides radically reducing the subsequent data-handling costs, such a compression can allow a better physical understanding of the nature of the navigational information in each pass. Such understanding is useful in allocating other system errors and in efficiently predicting navigational accuracies over a spectrum of mission situations.

It has been shown by J. O. Light (*SPS 37-33*, Vol. IV, pp. 8–16) that the "velocity parallax" due to the tracking station's rotation with the Earth is the most powerful factor in the doppler information for redetermining the orbit following a midcourse maneuver relatively near the Earth. In this article, it is established that a full pass of doppler data can meaningfully be interpreted as measuring the probe's mean geocentric *radial velocity*, its *right ascension*, and the cosine of its *declination*. For many mission situations, the latter two angles are extremely important in the navigational accuracies attainable. Thus the importance of tracking relatively near to the horizon is established since the accuracy of the right ascension and declination determinations is critically dependent on the fraction of the full pass included in the tracking. Subsequent articles will deal with this subject in greater depth and will treat other data noise models than the conservative one used here.

2. Calculation of the Observable

In Fig. 14, the observer (tracking station) is rotating about the z-axis at a distance of r_s with an angular rate ω. The probe, P, has coordinates $\mathbf{r}$ and $\dot{\mathbf{r}}$ relative to the x-y-z inertial frame. Since we are dealing with a distant probe, $r_s/r << 1$ and $z_0/r << 1$. The range from observer to the probe, ρ, is obtained from

$$\rho^2 = (x - r_s \cos\theta)^2 + (y - r_s \sin\theta)^2 + (z - z_0)^2. \qquad (1)$$

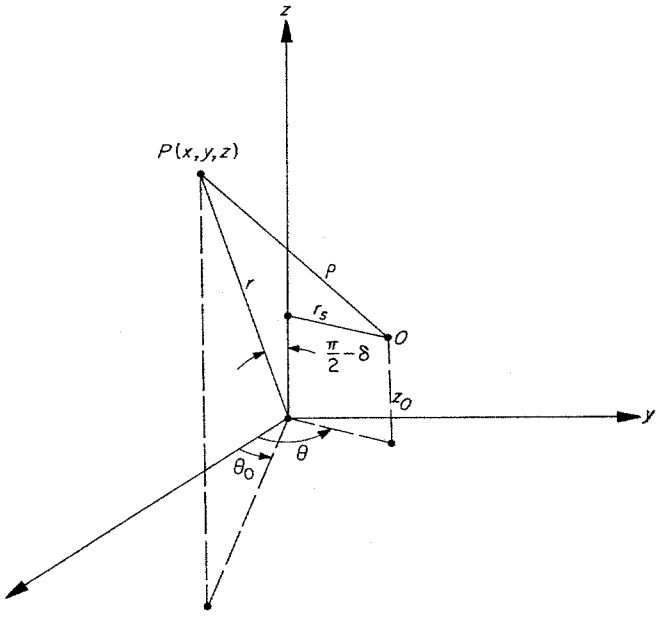

Fig. 14. Coordinates of probe, P, and observer, O

The range rate is composed of two parts, the motion of P and the motion of O; hence

$$\dot{\rho} = \frac{\partial \rho}{\partial t} + \frac{\partial \rho}{\partial \theta}\frac{d\theta}{dt}$$

or

$$\rho\dot{\rho} = (x - r_s\cos\theta)(\dot{x} + \omega r_s \sin\theta) + (y - r_s\sin\theta)(\dot{y} - \omega r_s\cos\theta) + \dot{z}(z - z_0) \qquad (2)$$

By expanding in powers of r_s/r and z_0/r, we obtain the following expression

$$\dot{\rho} = \dot{r} + \omega r_s\left(\frac{x}{r}\sin\theta - \frac{y}{r}\cos\theta\right) + \frac{r_s}{r}\left[\dot{r}\left(\frac{x}{r}\cos\theta + \frac{y}{r}\sin\theta\right) - \dot{x}\cos\theta - \dot{y}\sin\theta - \omega r_s\left\{\frac{xy}{r^2}\cos 2\theta + \left(\frac{y^2 - x^2}{r^2}\right)\frac{\sin 2\theta}{2}\right\}\right]$$
$$+ \frac{z_0}{r}\left[\frac{z}{r}\left\{\dot{r} + \omega r_s\left(\frac{x}{r}\sin\theta - \frac{y}{r}\cos\theta\right)\right\} - \dot{z}\right] + 0\left[\frac{r_s^2}{r^2}, \frac{z_0 r_s}{r^2}, \frac{z_0^2}{r^2}\right]. \quad (3)$$

The observed $\dot{\rho}$ is given by the geocentric range rate, $\dot{r}$, plus a term of the form

$$\frac{r_s\,\omega \cdot (\mathbf{r} \times \mathbf{r}_s)}{r r_s}$$

($r_s\omega$ is about 400 m/sec for a 30 deg latitude station), plus terms in the small parameters r_s/r, z_0/r. For a probe at $r = 0.03$ AU, these small parameters are about 10^{-3}. It is our intent to show that the expression below, obtained by letting $r \to \infty$ in Eq. (3), exhibits the important characteristics necessary to an understanding of the information content in a pass of doppler tracking data;

$$\dot{\rho} = \dot{r} + \omega r_s \cos\delta \sin(\theta - \theta_0), \text{ where } \theta - \theta_0 = \omega(t - t_0). \quad (4)$$

In calculations with real data, no such approximations are made. The subsequent error analysis uses (4) because it is a simple and remarkably accurate description of the real situation.

3. Regression Analysis

The precision to which the right ascension, declination and geocentric radial velocity of the probe can be obtained from a single pass of data will now be described.

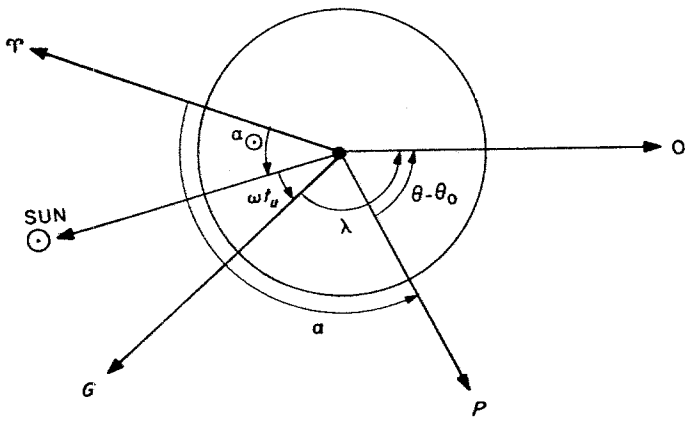

Fig. 15. Equatorial projection of coordinates in Fig. 14

Our basic data equation in (4) has been expressed in terms of the observable $\dot{\rho}$ and the angle θ. It is convenient to express θ in terms of the measurable quantity universal time, t_u, which determines the instantaneous angular orientation of the Earth about its axis of rotation. From Fig. 14 we note that θ is measured in the equatorial plane. From the equatorial projection in Fig. 15 it follows that $\theta - \theta_0$ is given by

$$\theta - \theta_0 = \omega t_u + \alpha_\odot + \lambda - \alpha \quad (5)$$

where

- ♈ is the mean vernal equinox of 1950.0,
- $\alpha_\odot$ is the instantaneous right ascension of the mean Sun,
- ω is the mean rotation rate of the Earth of date,
- t_u is the true universal time,
- λ is the longitude of the observer O measured in an easterly direction from Greenwich,
- α is the instantaneous right ascension of the space probe, P.

The right-hand members of (5) have error components of diverse size, and so it is important that we describe our assumptions concerning each of these errors. The quantity ω is assumed to be known exactly. There are, of course, stochastic fluctuations in ω which lead to changes in the rate of t_u as measured by a "Newtonian" clock; however, from observational data on this fluctuation it may be shown that the accumulated effect of an error in ω over one pass has a negligible effect relative to other error sources. The quantity t_u is approximated by the so-called $UT.1$ time which is the best estimate of true universal time. We assume that $UT.1$ is measured exactly but that it has an unknown stochastic error ξ, which is probably less than $0^s.002$ and effectively constant over one pass. We assume that $\alpha_\odot$ is known exactly. The longitude of the observer is assumed to have a small unknown bias ε_λ. In addition, the distance of O off the spin axis r_s, is assumed to have a small unknown bias ε_{r_s}.

The problem is to find α, δ and $\dot{r}$ at the instant P crosses the meridian of $O(\theta = \theta_o)$ and to find the precision in the estimates of these quantities in the presence of data noise, the timing error ξ, and the small unknown biases in λ and r_s. We assume here that $\dot{\mathbf{r}}$, α and δ are constant over one pass, and that $|\dot{\mathbf{r}}|/\omega r << 1$, $r_s/r << 1$, and $z_o/r << 1$, so that the simplified data expression in (4) is valid. Later reports will deal with the additional information gained from the small departures from these assumptions which occur in actual missions.

In order to put our data equation in a convenient form for regression analysis, we define the quantity α^* to be a specified value of the right ascension of $P(x, y, z)$ which from a-priori information is known to be near the true value, α. The small quantity ε_α given by $\varepsilon_\alpha = \alpha - \alpha^*$ is to be determined from measurements. Similarly, we define λ^* to be the a-priori value of the longitude of O and ε_λ is given by $\varepsilon_\lambda = \lambda - \lambda^*$. We also define $\xi = t_u - t_u^*$, where t_u is the true universal time, and t_u^* is $UT.1$. Next, we define t by the relation

$$\omega t = \omega t_u^* + \alpha_\odot + \lambda^* - \alpha^* \tag{6}$$

We note that t is an observable. The equation for θ in (5) now becomes

$$\theta - \theta_o = \omega(t - t_o) \tag{7}$$

where t_o is given by

$$\omega t_o = \varepsilon_\alpha - \varepsilon_\lambda - \omega\xi \tag{8}$$

Our a-priori choices for α, λ and t_u are such that ωt_o is a small quantity which is to be estimated from the observations.

Since ωt_o is small, using (4) and (8), the data equation becomes

$$\dot{\rho} = a + b \sin \omega t + c \cos \omega t + n(t) \tag{9}$$

where

$$a = \dot{r},$$

$$b = r_s \omega \cos\delta \cos \omega t_o \doteq r_s \omega \cos\delta,$$

$$c = r_s \omega \cos\delta \sin \omega t_o \doteq \omega t_o r_s \omega \cos\delta$$

and $n(t)$ is the data noise. We assume that a pass is symmetric about $t = t_o \approx 0$ and that N observations are made at equally spaced time intervals over the pass. Further, we assume white gaussian noise of mean zero and variance $\sigma_{\dot{\rho}}^2$. The maximum likelihood estimates of a, b and c are given by

$$\hat{a} = \frac{1}{2\psi(1 - \rho_{13}^2)}\left[\int_{-\psi}^{\psi} \dot{\rho}(\phi)\, d\phi - \frac{2\sin\psi}{\psi\left(1 + \frac{1}{2\psi}\sin 2\psi\right)}\int_{-\psi}^{\psi} \dot{\rho}(\phi)\cos\phi\, d\phi\right] \tag{11}$$

$$\hat{b} = \frac{1}{\psi\left(1 - \frac{1}{2\psi}\sin 2\psi\right)}\int_{-\psi}^{\psi} \dot{\rho}(\phi)\sin\phi\, d\phi \tag{12}$$

$$\hat{c} = \frac{1}{2\psi(1 - \rho_{13}^2)}\left[\frac{2}{\left(1 + \frac{1}{2\psi}\sin 2\psi\right)}\int_{-\psi}^{\psi} \dot{\rho}(\phi)\cos\phi\, d\phi - \frac{2\sin\psi}{\psi\left(1 + \frac{1}{2\psi}\sin 2\psi\right)}\int_{-\psi}^{\psi} \dot{\rho}(\phi)\, d\phi\right] \tag{13}$$

where ψ is the half-width of the pass, i.e., $-\psi \leq \theta \leq \psi$. Here, we have replaced the summations in our discrete process by integrations since N is in practice large and since we are not interested in an actual evaluation of the constants. We observe that due to our assumption of a symmetric pass with $t_o \approx 0$, $\hat{b}$ is uncorrelated with $\hat{a}$ and $\hat{c}$

but that $\hat{a}$ and $\hat{c}$ are strongly correlated. In fact, the covariance matrix Λ of these estimates is given by

$$\Lambda = \begin{pmatrix} \dfrac{1}{1-\rho_{13}^2} & 0 & \dfrac{-2\sin\psi}{\psi\left(1+\dfrac{1}{2\psi}\sin 2\psi\right)(1-\rho_{13}^2)} \\ 0 & \dfrac{2}{\left(1-\dfrac{1}{2\psi}\sin 2\psi\right)} & 0 \\ \dfrac{2\sin\psi}{\psi\left(1+\dfrac{1}{2\psi}\sin 2\psi\right)(1-\rho_{13}^2)} & 0 & \dfrac{2}{\left(1+\dfrac{1}{2\psi}\sin 2\psi\right)(1-\rho_{13}^2)} \end{pmatrix} \frac{\sigma_{\dot{\rho}}^2}{N} \tag{14}$$

where ρ_{13} is the correlation between $\hat{a}$ and $\hat{c}$ and given by

$$\rho_{13} = \frac{-2^{1/2}\sin\psi}{\psi\left[1+\dfrac{1}{2\psi}\sin 2\psi\right]^{1/2}} \tag{15}$$

Note that for $0 \leq \psi \leq \pi/2$, ρ_{13} lies in the range $-1 \leq \rho_{13} \leq -0.9$ which reflects the non-orthogonality of the even-functions 1 and $\cos\phi$ over intervals symmetric about $\phi = 0$.

Fig. 16 shows the variation of the precision of these estimates with the half-width of the pass ψ. Notice that as ψ is reduced from 90 deg, the precisions of $\hat{a}$ and $\hat{c}$ are severely degraded whereas the precision of $\hat{b}$ deteriorates more gradually. These phenomena are easily explained from an examination of (9). Notice that $\hat{a}$ and $\hat{c}$ for small ψ are difficult to separate. The dashed curve gives the precision of $\hat{c}$ when a is assumed perfectly known. This case may be obtained from (14) by setting $\rho_{13} = 0$ and will be referred to in the sequel. Notice for this special case that $\sigma_{\hat{c}}$ remains relatively flat compared to $\sigma_{\hat{b}}$ and for small ψ, $\sigma_{\hat{b}}$ is substantially degraded relative to $\sigma_{\hat{c}}$. Again, (9) shows that an error in b is most easily seen at $\omega t = \psi = 90$ deg whereas the effect of an error in c is maximized at $\omega t = 0$.

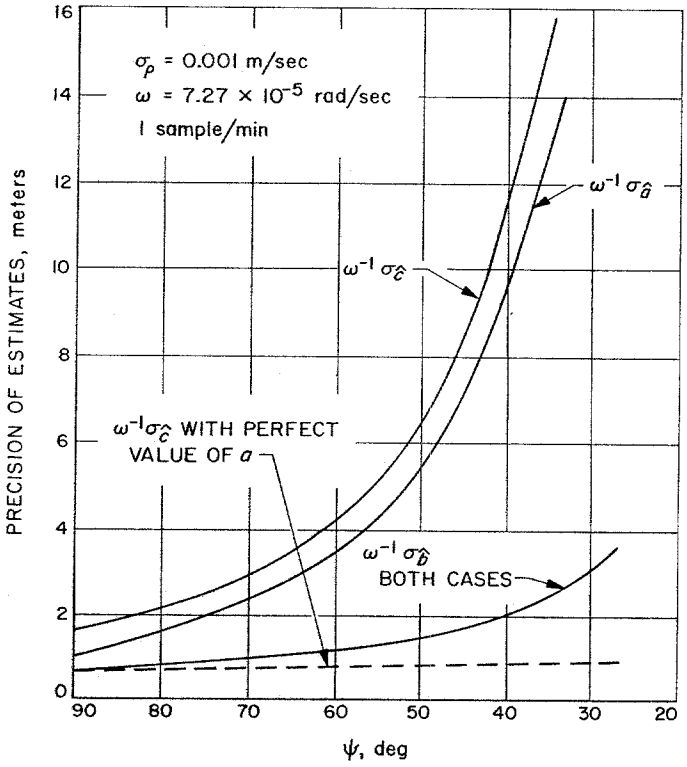

Fig. 16. Precision of parameter estimates $\hat{a}$, $\hat{b}$, $\hat{c}$, with half-width of pass ψ

The determination of $\dot{r}$ follows directly from a. For α, we have from (10) that

$$\omega\hat{t}_o = \hat{c}/\hat{b} \tag{16}$$

and it follows since $\hat{c}$ and $\hat{b}$ are uncorrelated that the variance of ωt_o is given by

$$\sigma^2_{\omega\hat{t}_o} = \hat{b}^{-2}\sigma_{\hat{c}}^2 + (\omega\hat{t}_o)^2 b^{-4}\sigma_b^2 \doteq \hat{b}^{-2}\sigma_{\hat{c}}^2 \tag{17}$$

since ωt_o is near zero. The estimate for α now follows from (8) provided ε_λ and ξ are given.

Since ξ, ε_λ, and t_u are uncorrelated, it follows from (8) that the variance of $\hat{\alpha}$ is given by

$$\sigma_{\hat{\alpha}}^2 = \sigma^2_{\omega\hat{t}_o} + \omega^2\sigma_\xi^2 + \sigma_\lambda^2 \tag{18}$$

From the coefficient $\hat{b}$, we obtain an estimate of $\cos\delta$ provided r_s is given. Further, the variance of $\hat{\delta}$ is given by

$$\sin^2\hat{\delta}\,\sigma_{\hat{\delta}}^2 = (r_s\omega)^{-2}\,\sigma_{\hat{b}}^2 + r_s^{-2}\cos^2\hat{\delta}\,\sigma_{\dot{r}_s}^2 \qquad (19)$$

Finally, the correlation in $\hat{a}$ and $\hat{c}$ is easily removed by choosing a linear combination of these quantities which diagonalizes the covariance matrix Λ. The magnitudes of the eigenvectors, $\hat{a}'$, $\hat{b}'$, $\hat{c}'$, are given by

$$\begin{cases} \hat{a}' = \hat{a}\cos\Gamma + \hat{c}\sin\Gamma \\ \hat{b}' = \hat{b} \\ \hat{c}' = \hat{c}\cos\Gamma - \hat{a}\sin\Gamma \end{cases} \qquad (20)$$

where Γ is found to be

$$\tan 2\Gamma = \frac{-4\sin\psi}{\psi\left(1 - \frac{1}{2}\sin 2\psi\right)} \qquad \left(0 \leq -\Gamma \leq \frac{\pi}{2}\right) \qquad (21)$$

Note that $45° \leq -\Gamma \leq 56°$ for $0 \leq \psi \leq 90°$. The eigenvalues $\sigma_{a'}{}^2$, $\sigma_{b'}{}^2$, and $\sigma_{c'}{}^2$ are given by

$$\begin{cases} \sigma_{\hat{a}'}{}^2 = \dfrac{\sigma_{\hat{a}}^2 + \sigma_{\hat{c}}^2}{2} + \dfrac{1}{2}\left[(\sigma_{\hat{a}}^2 - \sigma_{\hat{c}}^2)^2 + 4\sigma_{\hat{a}}^2\,\sigma_{\hat{c}}^2\,\rho_{13}^2\right]^{1/2} \\ \sigma_{\hat{b}'}{}^2 = \sigma_{\hat{b}}^2 \\ \sigma_{\hat{c}'}{}^2 = \dfrac{\sigma_{\hat{a}}^2 + \sigma_{\hat{c}}^2}{2} - \dfrac{1}{2}\left[(\sigma_{\hat{a}}^2 - \sigma_{\hat{c}}^2)^2 + 4\sigma_{\hat{a}}^2\,\sigma_{\hat{c}}^2\,\rho_{13}^2\right]^{1/2} \end{cases} \qquad (22)$$

Fig. 17 shows the behavior of these eigenvalues as a function of ψ. The effect of the correlation in $\hat{a}$ and $\hat{c}$ now is cast completely into $\sigma_{\hat{a}'}$. The precision of $\hat{c}$ goes as essentially $1/N^{1/2}$.

4. Interpretation of the Results

In Sec. 3 above, we concluded that the estimate of geocentric radial velocity of the probe and its precision follow directly from the coefficient $\hat{a}$ and its variance $\sigma_{\hat{a}}^2$. For the right ascension and declination, these determinations are not as straightforward, for we have seen that the precision of these determinations depends on our knowledge of the station location and also timing in the case of right ascension.

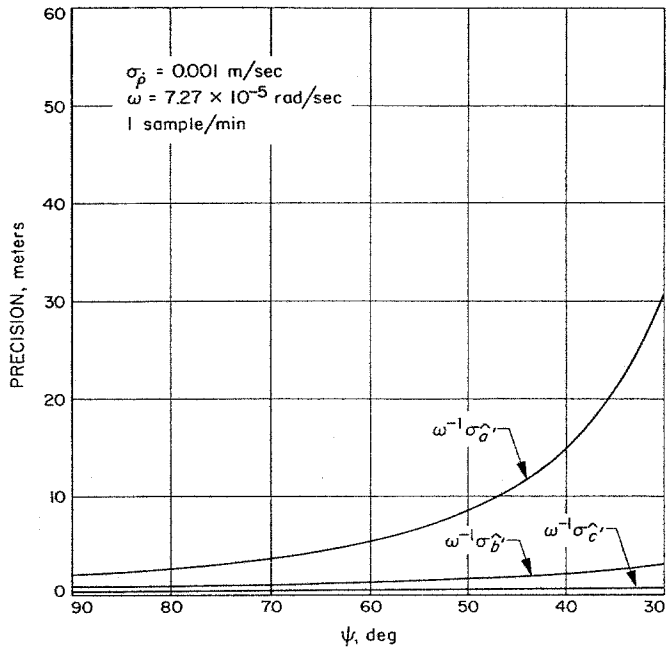

Fig. 17. Behavior of eigenvalues as a function of ψ

Let us first address ourselves to the problem of station location. We note in passing that (3) provides an explanation for the observed fact in actual missions that the component of the position of O parallel to the spin axis is not well determined nor, conversely, does a small error in this component seriously affect the results.

For the distance off the spin-axis r_s, it follows from (10) that r_s will be strongly determined for probe declinations near zero; in fact, for this case we have

$$\sigma_{r_s} = \omega^{-1}\,\sigma_{\hat{b}} \qquad (\delta = 0) \qquad (23)$$

Referring to Fig. 16, we see for a full pass ($\psi = 90°$) and for $\sigma_{\dot{\rho}} = 1$ mm/sec, that r_s is determined to 1 meter. Furthermore, in an actual mission the probe P is being accelerated by other bodies (e.g., the Sun) whose geocentric right ascensions and declinations are precisely known; this effect enables one to obtain a good separation of the instantaneous declination and the spin axis bias when observations are taken over a sufficiently wide span of the trajectory of P. In any case, a precision of 1 meter for r_s, for $\sigma_{\dot{\rho}} = 1$ mm/sec, emphatically demonstrates that in order to realize this precision, one must be careful to insure that all error sources of this magnitude are incorpoated in the mathematical model used in the actual orbit determination process. This includes such effects as antenna motion, nutation and wandering of the pole of the

Earth, tidal deformations of the Earth, and ionospheric effects.

In the case of station longitude bias, the problem is coupled with errors in universal time. An error of 0.002 in time is equivalent to about 1 meter in a longitude direction for the station. For two different stations on the surface of the Earth, the relative longitude is not affected by *UT*.1 errors provided they can synchronize the observations. As in the case of r_s determinations, if one knows the right ascension of P by "independent" means (e.g., from observations of a *Ranger* spacecraft near lunar impact) more precisely than ωt_0 can be determined, we obtain a strong determination of the bias in λ. For this case, it follows from (8) that

$$\sigma_\lambda^2 = \sigma_{\omega t_0}^2 + \omega^2 \sigma_\xi^2 \qquad (\varepsilon_\alpha = 0) \tag{24}$$

For, $\sigma_{\dot\rho} = 1$ mm/sec and $\sigma_\xi = 0.002$, $r_s \sigma_\lambda$ is about 2 meters. Here, we have used (17) to evaluate $\sigma_{\omega \hat{r}_0}$ from σ_ε using the $\psi = 90$ deg point on Fig. 16. If $\dot r$ of P also is predicted independently the value of $\sigma_{\dot\xi}$ should move toward the dashed curve in Fig. 16. Hence, we would ultimately expect λ to be determined to a precision commensurate with σ_ξ. Fig. 18 shows actual Goldstone-Woomera relative longitude determinations from *Rangers* 6–9. In these flights, software accuracy limitations cause $\sigma_{\dot\rho}$ to be degraded to about 10 mm/sec.

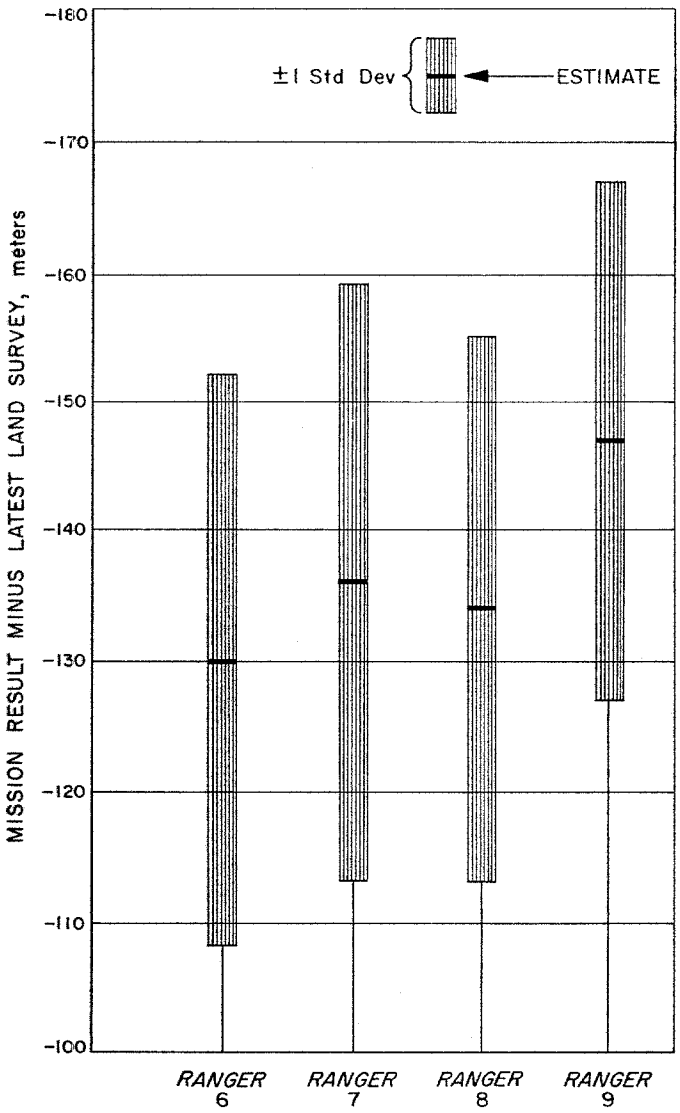

Fig. 18. Goldstone station location relative to longitude difference of Woomera, with time correction

Finally, if we assume that the station locations have become sufficiently well established so that the biases ε_λ and ε_{rs} are not the dominant error sources, it follows that (18) and (19) and Fig. 16 may be used to obtain the precision with which α and δ can be estimated from one pass of doppler data. The timing error also is not dominant provided $\sigma_{\dot\rho} \geqq 1$ mm/sec. Taking $\psi = 80$ deg and multiplying by $(2)^{1/2}$ to allow for the contingencies of timing and station location errors we have the result that

$$\sigma_\alpha = 5 \times 10^{-7} \text{ radians} \tag{25}$$

$$\sin \delta \sigma_\delta = 2.5 \times 10^{-7} \text{ radians} \tag{26}$$

These accuracies are equivalent to about 0.″1 arc which is similar to the accuracy of angular data obtained from astronomical observations. In addition, $\dot r$ is determined to

$$\sigma_{\dot r} = 0.1 \text{ mm/sec} \tag{27}$$

Hardware performance in the near future will have accuracies of better than $\sigma_{\dot\rho} = 1$ mm/sec, probably around 0.1 mm/sec. Although a more careful analysis of our limiting error sources is required for such systems, it is clear that it may be possible to significantly reduce the numbers in (25), (26), and (27).

Acknowledgments. The authors have benefited from many conversations with members of the Systems Analysis Section in arriving at the results described above. Particular acknowledgment is due to J. D. Anderson and J. O. Light.